Journal of the European Ceramic Society **15** (1995) 165–171
1995 Elsevier Science Limited
Printed in Great Britain

The Densification and Microstructural Development of Al_2O_3 with Manganese Oxide Addition

H. Erkalfa, Z. Mısırlı, M. Demirci, Ç. Toy & T. Baykara*

TUBITAK, Marmara Research Center, Materials Research Department, 41470 Gebze, Turkey

(Received 19 April 1994; accepted 5 July 1994)

Abstract

The effect of MnO_2 as an additive on the densification behaviour and microstructural evolution of α-Al_2O_3 has been investigated over a wide sintering regime. A colloidal technique was applied for the mixing of MnO_2 in order to achieve a uniform distribution and homogeneous microstructures. Sintered density, average grain size and microstructural features were elaborated along with the microhardness and mechanical strength measurements. Manganese oxide was found to promote grain growth and an intergranular second phase formation was detected for additions over 0·5 wt% MnO_2. Excessive grain growth and draining of the second phase were observed in the samples with 3 wt% MnO_2 additions sintered above 1500°C.

1 Introduction

Additives in small amounts are deliberately and commonly used in ceramic systems to influence densification processes either by reducing sintering temperature or suppressing/promoting grain growth or enhancing mechanical and physical properties. A variety of oxides such as MgO, TiO_2, SiO_2, MnO_2, Cr_2O_3, Fe_2O_3 are some of the typical additives that have been commonly used in alumina ceramics.[1–3] As examples, it is well known that small additions of MgO to Al_2O_3 reduce the grain growth rate, while Fe_2O_3 and TiO_2 additions were found to enhance sintering along with a grain growth. On the other hand, CaO and SiO_2 additions were found to be detrimental to the densification process, although they yielded finer grain size and distribution in the microstructures.[4–7]

Very few investigations have been conducted on the influence of manganese oxide additions for the initial sintering of alumina. However, examination of the microstructural features and development during the sintering and detailed analysis in the densification regime has not been reported yet. Considering the commercial importance of structural alumina components with manganese oxide addition as thread guides, o-rings, sealants and nozzles, there is a considerable lack of information and data on these compositions.

The influence of manganese oxide addition to alumina, according to the results of those earlier studies based on shrinkage data, was shown to accelerate the sintering rate and grain growth. Similar to the effect of TiO_2, the sintering rate increases to a maximum and then levels off and starts decreasing as the Mn concentration exceeds 0·3 wt%, presumably due to the formation of a second phase. However, in these studies the formation of the second phase particles was not experimentally verified.[8–13]

It was first proposed that the addition of MnO_2 in the proportion of 0·1–1·0 wt% caused a change in diffusion mechanism from a grain boundary process to a bulk diffusion process, which was also observed for the sintering of undoped alumina samples.[9] The rate-controlling mechanism for densification by both bulk and grain boundary diffusion is oxygen ion diffusion. In the case of MnO_2 addition in the sintering of Al_2O_3, Mn occupying a cation site increases the oxygen ion vacancy concentration. A gradient in Mn concentration results in a wide region of enhanced diffusion at the grain boundaries.

Earlier studies on the Al_2O_3–MnO_2 system did not examine the grain morphologies and it was claimed that there was no evidence of grain growth observed in the composition with 0·3 wt% MnO_2 sintered at 1600°C.[11,12] However, MnO_2 is known to greatly enhance grain growth. Discontinuous grain growth and the anisotropy of the grains, especially in the large grains in Al_2O_3 with addition of MnO_2, have been reported.[10] It was

* To whom correspondence should be addressed.

also argued in the earlier reports that manganese oxide forms a spinel and also goes into solid solution in the excess Al_2O_3 which brings about grain growth of alumina.[3]

The purpose of this study was to investigate the microstructural development and densification characteristics in the Al_2O_3–MnO_2 system in an extensive sintering and composition regime using varying amounts of MnO_2 addition ranging between 0, 0·1, 0·3, 0·5, 1·0, 1·5 and 3·0 wt%. This report also discusses the measured microhardness values and strength data of the samples with respect to the microstructural features which developed at different sintering temperatures.

2 Experimental

In ceramic processing, a sufficient mixing of additives and major powders is absolutely essential to obtain high quality, homogeneous mixtures. For this reason, colloidal techniques were employed in this study to prepare homogeneous batches of Al_2O_3—MnO_2 compositions. Alcoa A 16SG alumina powder with an average particle size of 0·37 microns and specific surface area of 9 m^2/g and reagent grade $Mn(CH_3COO)_2.4H_2O$ were used as the starting materials. The acetate of manganese can easily be dissolved in water to its ions to yield a homogeneous dispersion. For the preparation of alumina suspensions with addition of 0·1, 0·3, 0·5, 1·0, 1·5, and 3·0 wt% MnO_2, manganese (2) acetate was dissolved in water and its pH adjusted to 2 with formic acid and HCl. As alumina powder is gradually added into the water–acetate solution, continuous magnetic stirring and ultrasonicating were applied to the suspension to break up the agglomerates. Colloidal suspensions with 0·1, 0·3, 0·5 and 3·0 wt% MnO_2 were oven-dried at 90–110°C for 12 h and mixed regularly to prevent sedimentation. Colloidal suspensions with 0·5, 1·0 and 1·5 wt% MnO_2 additions were freeze-dried in order to obtain soft agglomerates which form due to capillary forces between the particles during the removal of frozen solvent by sublimation. Powders dried using both oven and freeze drying were calcined at 600°C for 1 h in order to obtain insoluble oxides of the additives.

Powder compacts were prepared using the dry, uniaxial pressing technique in a steel die to make pellets nominally 2–2·5 cm in diameter and 0·3 cm in height, applying a pressing stress of 100 MPa. Freeze-dried powders were pressed into a bar shape and these samples were further isostatically cold pressed at 300 MPa. For the purpose of comparison, undoped alumina powders and pellets were also prepared using the same techniques as those applied to MnO_2-added samples. Green densities of the samples were measured dimensionally. For the compositions with 0·1, 0·3 and 0·5 wt% MnO_2 the sintering regime of 1550, 1600 and 1650°C for 1 h is selected for densification, whereas in the case of 1·0 and 1·5 wt% MnO_2 additions, the sintering temperature was selected to be 1550°C for 2 h sintering hold period. For the undoped and doped samples with 3 wt% MnO_2, sintering at temperatures ranging 1250 to 1650°C for 1 h were performed. In all cases the sintering was done under normal furnace atmospheric conditions at a heating rate of 5–10°C/min and cooled at the same rate in the furnace atmosphere.

After sintering, sample densities were determined by the water immersion technique. The microstructure of the samples were studied by scanning electron microscopy (SEM) equipped with an energy dispersive X-ray spectrometer (EDS) attachment on polished and thermally etched surfaces. Vickers microhardness values were measured with a Leitz Mini Load Hardness Tester and a Shimadzu Microhardness Tester (Type M) by applied loads E of 200, 300 and 500 g. The average of 10–20 indentations per specimen was taken. The average mechanical strength of samples was calculated using the failure loads of samples determined from a ball-on-ring test and a tensile testing apparatus (Instron, model 1115) equipped with a three-point loading system.

3 Results and discussion

Compositions, the percentage of the theoretical density attained after sintering and the average grain size values which were determined using standard line intercept technique are tabulated in Table 1. As explained before, the data and micrographs for undoped alumina samples are also presented for the purpose of comparison. The sintered densities of the samples were found to be between 98–99% of the theoretical densities with insignificant differences between the sintering temperatures of 1550–1650°C.

As can be seen in the micrographs given in Fig. 1, undoped alumina can be sintered to its full density at temperatures above 1550°C, during which a relatively homogeneous grain growth occurs and only a few pores are retained between the grains. The average grain size is increased to 3·05 microns after sintering at 1650°C for 1 h. As shown in Fig. 2, 0·1 wt% MnO_2 addition led to inhomogeneous grain growth after sintering at 1600°C for 1 h, resulting in a microstructure with localized regions of finer grains around larger sized grains. Further addition of MnO_2, 0·3–1·5 wt%, caused a drastic

Table 1. The percentage of theoretical density attained and grain size measurements as a function of MnO_2 (wt%) and the sintering conditions

MnO_2 (wt%)	Sintering conditions	Percentage theoretical density attained	Grain size (μm)
0·0 (undoped)	1250°C, 1 h	68·7	0·32
	1350°C, 1 h	77·1	0·33
	1450°C, 1 h	89·9	0·84 ± 0·04
	1550°C, 1 h	97·5	1·48 ± 0·25
	1600°C, 1 h	99·5	
	1650°C, 1 h	100	3·05
0·1	1550°C, 1 h	98·0	
	1600°C, 1 h	99·0	2·74 ± 0·28
	1650°C, 1 h	99·2	
0·3	1550°C, 1 h	98·0	
	1600°C, 1 h	98·5	13·9 ± 3·73
	1650°C, 1 h	99·2	
0·5	1550°C, 1 h	98·2	7·5 ± 2·88
	1600°C, 1 h	98·0	17·2 ± 6·01
	1650°C, 1 h	98·5	25·1 ± 6·42
0·5	1550°C, 2 h	98–99	20·55 ± 4·14
1·0	1550°C, 2 h	98–99	19·29 ± 2·79
1·5	1550°C, 2 h	98–99	17·87 ± 1·69
3·0	1250°C, 1 h	73·0	0·51
	1350°C, 1 h	86·3	0·84 ± 0·03
	1450°C, 1 h	96·2	1·34 ± 0·14
	1550°C, 1 h	98·7	13·84 ± 10·23

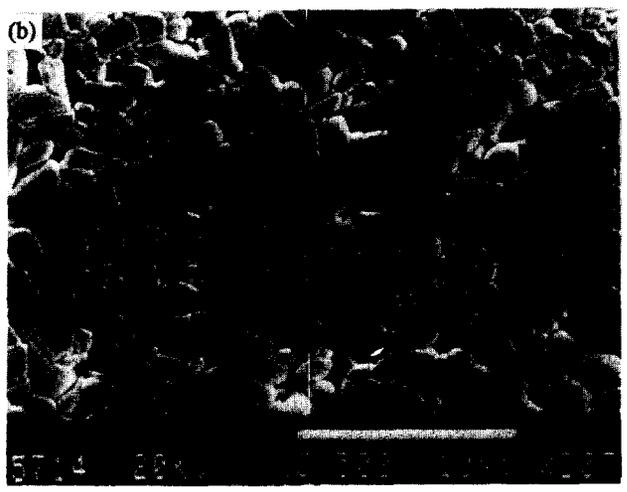

Fig. 1. SEM micrographs of undoped alumina samples after sintering (a) at 1550°C for 1 h and (b) at 1650°C for 2 h.

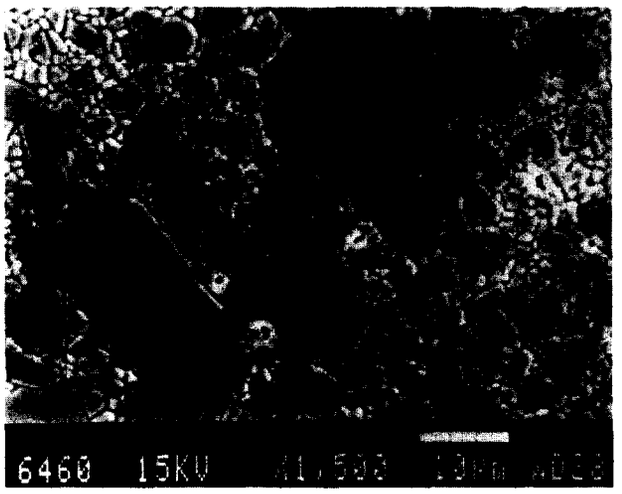

Fig. 2. SEM micrograph of 0·1 wt% manganese-doped alumina after sintering at 1600°C for 1 h.

change in the microstructures after sintering at 1550–1650°C, exhibiting exaggerated grain growth with grains as big as 25–100 microns (Figs. 3–5). A considerable amount of both inter- and intragranular pores is observed in the microstructure. At and above 0·5 wt% MnO_2 additions, less than one micron sized fine pores trapped inside the grains become more evident with sintering hold times of 2 h at 1550°C. In these micrographs (Figs. 4–6), elongated grains of up to 100 microns in length exist to yield irregular grain shapes with faceted morphologies. Furthermore, in these samples, a second phase exists as an intergranular grain boundary phase covering most of the grain boundary area, which is presumably in liquid form at the sintering temperature. It appears that this intergranular phase was distributed along the grains both as a continuous layer and in irregular forms (Fig. 7). According to the phase diagram given in Fig. 8, an eutectic composition is present in the MnO_2-rich side of the binary MnO_2–Al_2O_3 system at 1520°C. This grain boundary phase is

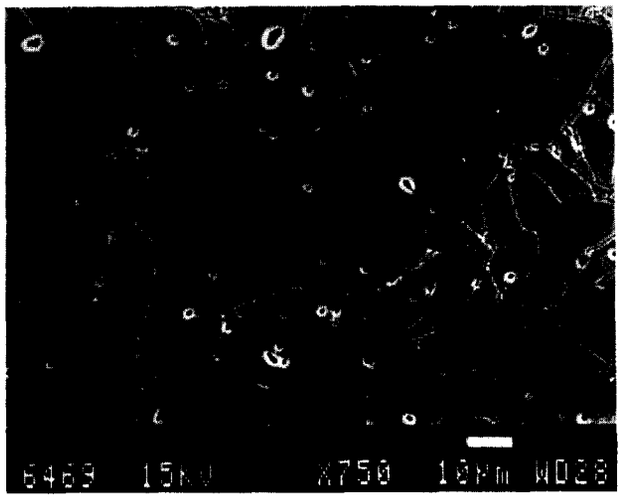

Fig. 3. SEM micrograph of 0·3 wt% manganese-doped alumina after sintering at 1600°C for 1 h.

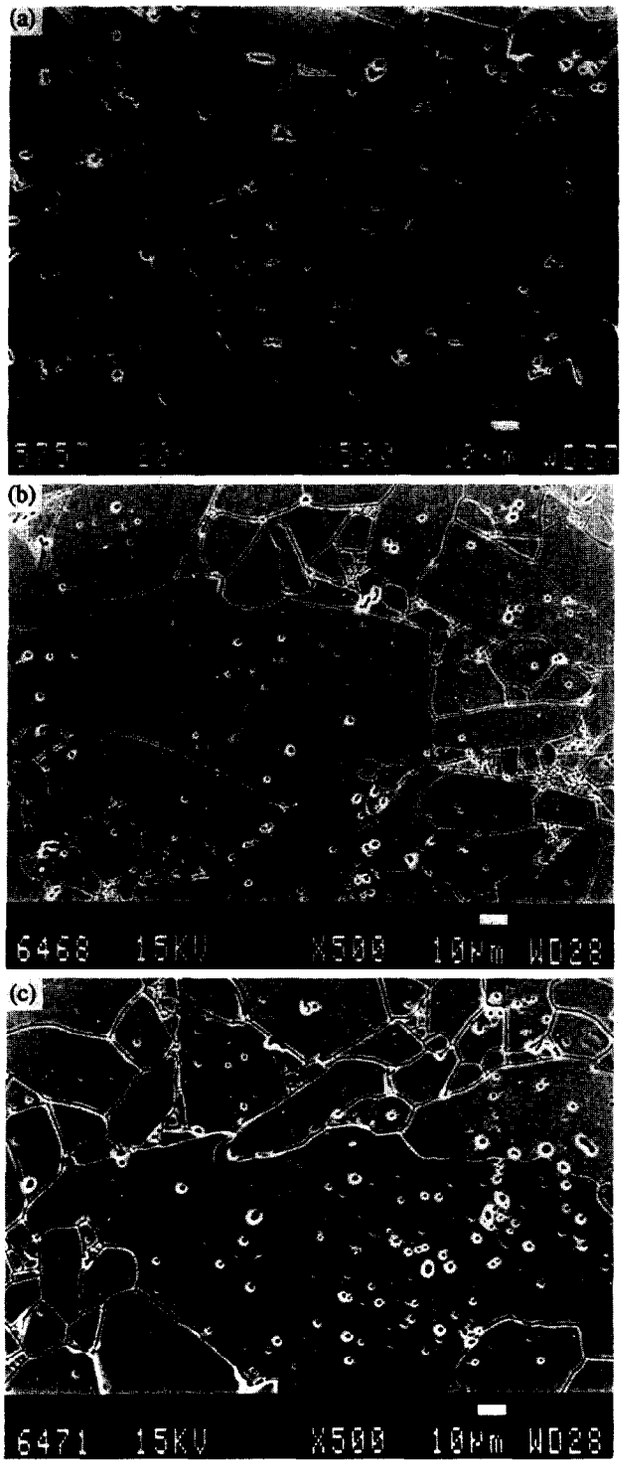

Fig. 4. SEM micrographs of 0·5 wt% manganese-doped alumina after sintering (a) at 1550°C for 2 h, (b) at 1600°C for 1 h and (c) at 1650°C for 1 h.

found to be Mn- and Ca-rich as analysed by the point analysis of energy dispersive X-ray spectroscopy (EDS) (Fig. 9).

In the earlier investigations, the shrinkage data was evaluated to show that bulk and boundary diffusion both are effective for the initial stage of sintering up to 4% shrinkage.[11,12] However, no detailed study was presented for the later stage of sintering. The micrographs shown in Figs. 2–4 for the samples with 0·1–0·5 wt% MnO_2 addition sintered at 1550–1650°C for 1 h do not indicate

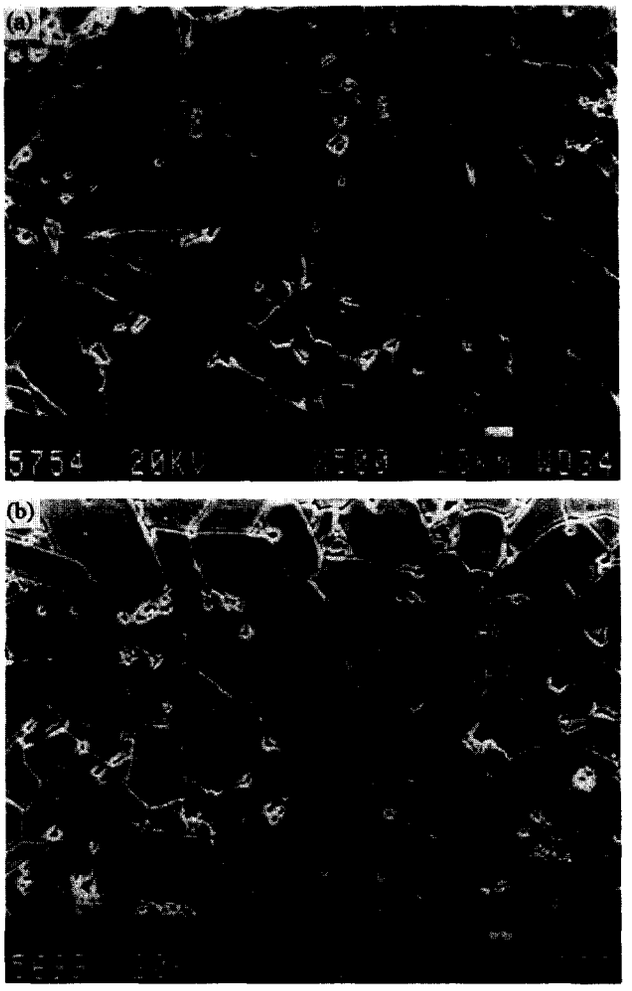

Fig. 5. SEM micrographs of manganese-doped alumina after sintering at 1550°C for 2 h; (a) 1·0 wt% and (b) 1·5 wt% manganese.

the presence of any grain boundary phase formation between the grains. Intergranular grain boundary phase was detected between the grains in those samples with 0·5–1·5 wt% MnO_2 additions sintered at 1550°C for 2 h. Based on these observations, the volume or grain boundary diffusion mechanism acts as the controlling process according to the composition and the sintering conditions during the later stages of densification.

It appears that the densification in compositions with 0·1–0·5 wt% MnO_2 additions sintered at 1550–1650°C for 1 h is enhanced via the volume diffusion process rather than the formation of an intergranular liquid phase. Manganese, like iron, displays variable valency, so that complex series of oxides and hydroxides exist. The ready valency change of manganese leads to many defect structures and non-stoichiometric compounds. Therefore, it may be suggested that different manganese cations with different valency states can substitute the Al cation sites within the crystalline structure, resulting in either vacancy formation or an extra electron. This type of phenomenon was shown to exist during sintering in the case of TiO_2 doping of alumina by activating the volume diffusion rate of

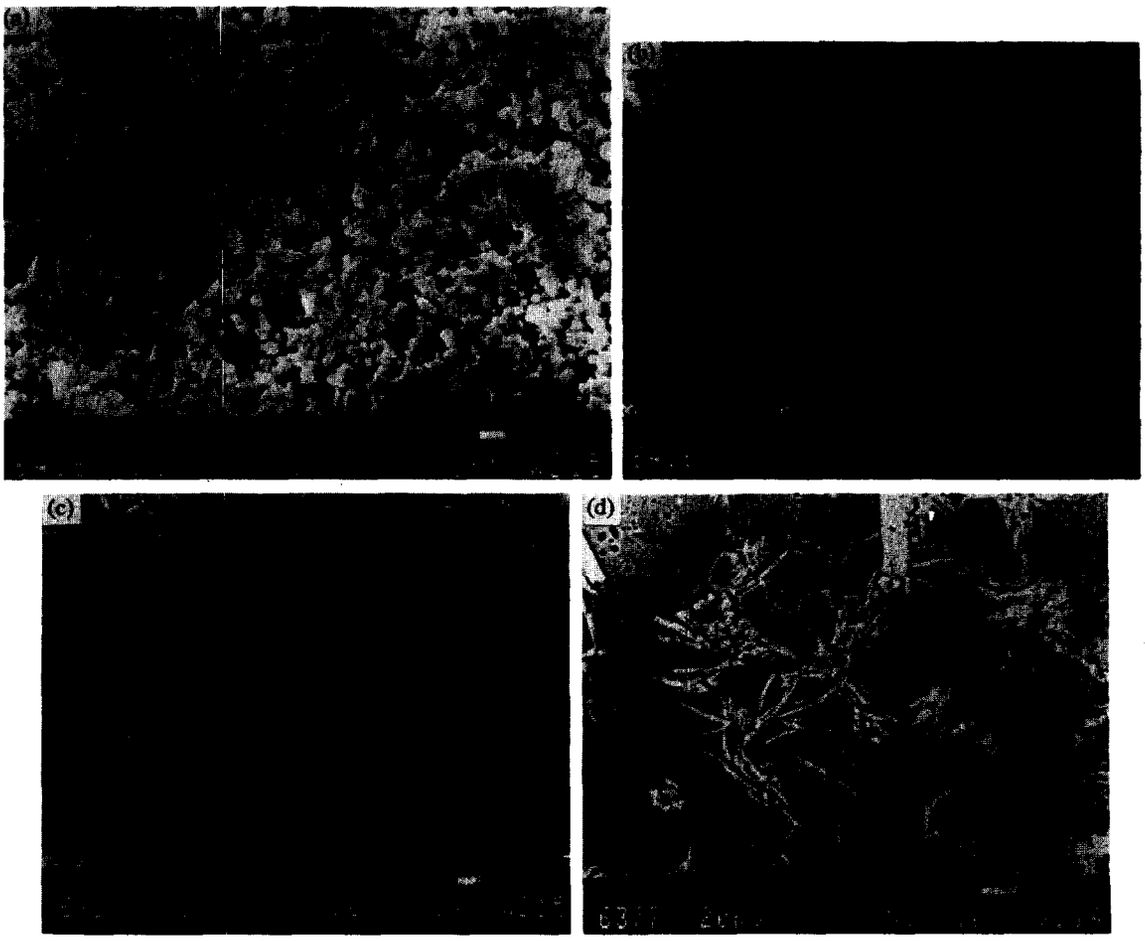

Fig. 6. SEM micrographs of 3·0% manganese-doped alumina after sintering (a) at 1250°C for 1 h, (b) at 1350°C for 1 h, (c) at 1450°C for 1 h, (d) at 1550°C for 1 h.

species[15]. The sintering rate is proportional to the vacancy concentration that forms as Ti^{+3} and Ti^{+4} enters Al_2O_3 substitutionally, and when the charge neutrality is being achieved by the presence of other divalent cations in the powder. In the earlier studies, suggested evaluation of the sintering data indicated that Mn, which substitutes Al in the alumina lattice, can be present in its Mn^{+2} and Mn^{+3} form and thus creates oxygen vacancies to increase diffusion coefficient. An energy dispersive X-ray analysis that was carried out on polished and thermally etched samples in SEM indicated that manganese was well distributed throughout the grains, and no segregation of manganese was detected at the grain boundaries (Fig. 10). Therefore, it may be elaborated that manganese cations substitute the Al sites, resulting in fast diffusion paths within the single grains during the sintering process. As a result of the faster diffusion paths formed, the process of excessive grain growth is enhanced when the amount of manganese oxide addition is between 0·1–0·5 wt% (Figs 2–4).

On the other hand, in the compositions with 1–1·5 wt% MnO_2 addition sintered at 1550°C for 2 h the presence of a secondary intergranular phase both in the form of continuous layer and irregular shapes indicates that the controlling mechanism is due to to grain boundary diffusion process (Fig. 7).

A wide range of sintering regimes, 1250–1550°C for 1 h, was studied on those samples with 3 wt% MnO_2. As shown in Fig. 6, the degree of densification can be observed in the micrographs sintered at 1250; 1350, 1450 and 1550°C for 1 h. In these samples, sintering up to 1450°C indicates a regular densification (73% to 96·2% of the theoretical density) and grain growth (0·51 to 1·34 microns) behaviour, whereas the micrographs for the samples sintered at 1550°C (Fig. 6) exhibits an abnormal and discontinious grain growth (up to 100 microns) with large number of pores trapped inside the grains. Such an abnormal and discontinious grain growth during the late stage of sintering leads to grain boundaries breaking away from the pores, resulting in excessive pore formation inside these newly formed large grains. These pores trapped inside the grains enlarge the diffusion distance to the next grain boundary to inhibit densification. Elimination of such pores is difficult. In these micrographs, the Mn-rich second phase seems to be squeezed out of the grain boundaries in needle-like shapes. Such a draining away from the grain boundaries justified the conclusion that a eutectic liquid phase formed between the grains.

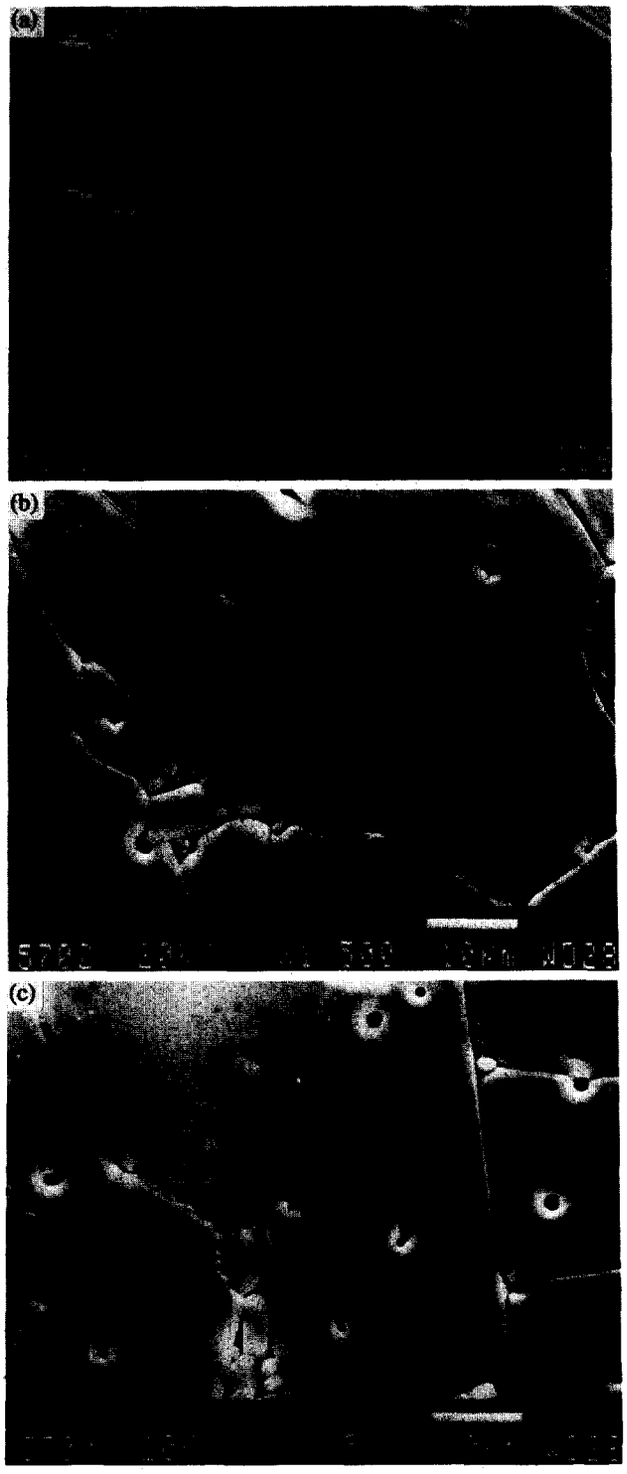

Fig. 7. Interganular second phase formation in the samples sintered at 1550°C for 2 h; (a) 0·5 wt%, (b) 1·0 wt% and (c) 1·5 wt% manganese.

Microhardness measurements and some of the strength data are presented in Table 2 as a function of sintering temperature and composition. It appears that there is an increase in microhardness values with sintering temperature and there is a slight increase with the manganese oxide additions. Microhardness measurements showed considerable variation and scatter for the compositions with 0·5 (sintered at 1550°C for 2 h, 1·0, 1·5 and 3·0 wt% MnO_2 additions, presumably due to formation of the softer second phase. It is difficult

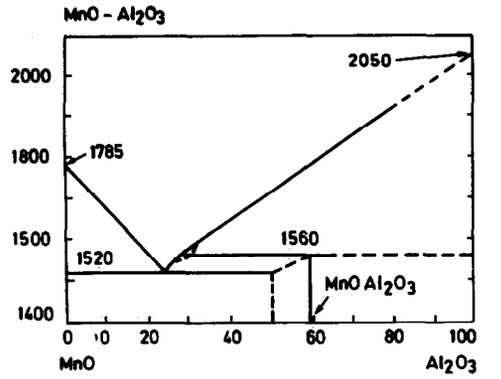

Fig. 8. The phase diagram of $MnO–Al_2O_3$ system.[14]

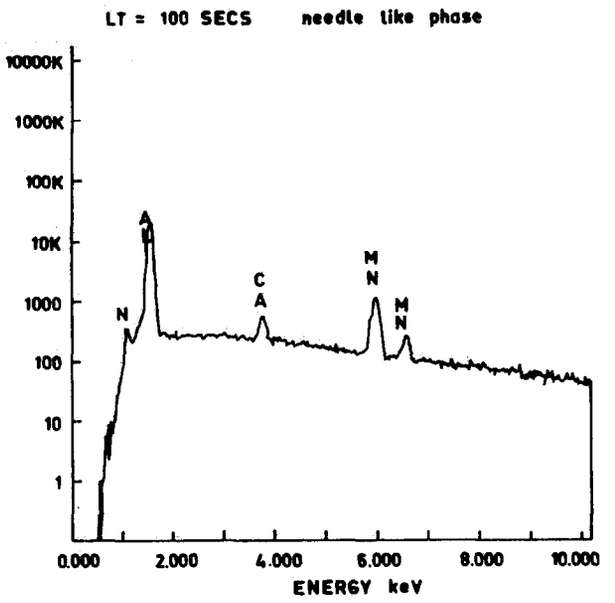

Fig. 9. Energy dispersive X-ray point analysis of the grain boundary phase.

Table 2. The microhardness measurements and strength data as a function of MnO_2 (wt%) and the sintering conditions.

MnO_2 (wt%)	Sintering conditions	Microhardness (GPa)	Strength (MPa)
0·0 (undoped)	1250°C, 1 h	—	—
	1350°C, 1 h	18·23 ± 1·56	—
	1450°C, 1 h	20·59 ± 1·27	—
	1550°C, 1 h	18·98 ± 0·64	344 ± 76·9
	1600°C, 1 h	19·41 ± 0·58	363 ± 53·2
	1650°C, 1 h	20·29 ± 0·85	334 ± 71·7
0·1	1550°C, 1 h	18·94 ± 0·44	299 ± 45·4
	1600°C, 1 h	19·36 ± 0·38	318 ± 37·6
	1650°C, 1 h	20·15 ± 0·63	296 ± 49·4
0·3	1550°C, 1 h	18·33 ± 0·72	239 ± 21·8
	1600°C, 1 h	18·86 ± 0·67	203 ± 16·7
	1650°C, 1 h	19·56 ± 0·55	380 ± 27·7
0·5	1550°C, 1 h	18·30 ± 0·79	200 ± 24
	1600°C, 1 h	18·80 ± 0·35	190 ± 20·3
	1650°C, 1 h	19·53 ± 0·42	353 ± 29·1
0·5	1550°C, 2 h	22·9 ± 1·60	439 ± 27
1·0	1550°C, 2 h	22·9 ± 0·77	453 ± 43
1·5	1550°C, 2 h	23·2 ± 1·56	465 ± 14
3·0	1250°C, 1 h	—	
	1350°C, 1 h	19·2 ± 2·03	
	1450°C, 1 h	21·4 ± 2·10	
	1550°C, 1 h	24·8 ± 2·67	

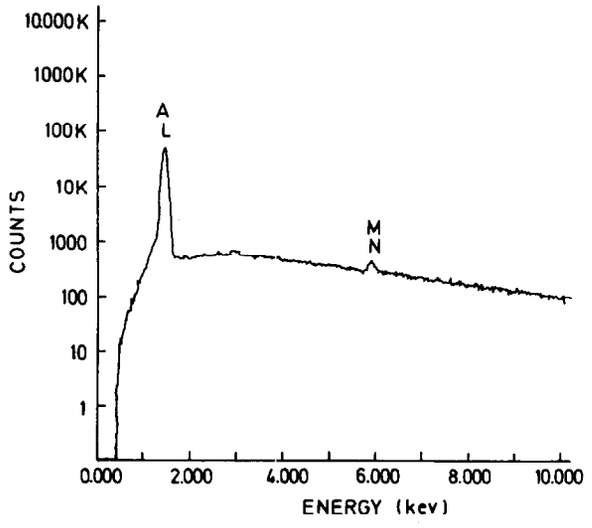

Fig. 10. Energy dispersive X-ray point analysis of the grain interior of 0·5 wt% MnO_2-doped Al_2O_3.

to derive definite information regarding the strength data given in this table; even the data shows higher strength values in the case above 0·5 wt% MnO_2 addition. It seems that further cold isostatic pressing of the samples with 0·5, 1·0 and 1·5 wt% MnO_2 sintered at 1550°C for 2 h led to such an increase in strength data. However, the scatter and variation in this set of data is at considerable level and should be interpreted cautiously.

4 Conclusion

The microstructural development of Al_2O_3 with MnO_2 addition was characterized at different sintering conditions. Grain growth was promoted with manganese oxide additions and in some cases due to prolonged sintering holds, an exaggerated grain growth behaviour was observed. It appears that the densification is controlled by a grain boundary diffusion mechanism in those samples with MnO_2 additions higher than 0·5 wt%. On the other hand, the volume diffusion mechanism is suggested to be the controlling process in the case of 0·1–0·5 wt% MnO_2 addition. Microhardness values and strength data do not reveal a definite trend; however, an increase in the microhardness values with temperature and the percentage MnO_2 were evident. Strength data also shows an increase with MnO_2 addition.

Acknowledgements

The authors acknowledge the support of NATO-SFS Programme for this study. The authors also thank Prof. Dr I. A. Aksay and F. Dogan of Princeton University for their contribution during the course of this investigation.

References

1. Rossi, G. & Burke, J. E., Influence of additives on the microstructure of sintered Al_2O_3. *J. Amer. Ceram Soc.*, **56** 1973 543–9.
2. Harmer, R. D., Roberts, E. W. & Brook, R. J., Rapid sintering of pure and doped α-Al_2O_3. *Trans. Brit. Ceram. Soc.*, **78** (1979) 22–5.
3. Smothers, W. J. & Reynolds, H. J., Sintering and grain growth of alumina. *J. Amer. Ceram. Soc.*, **37** (1954) 588–95.
4. Roy, S. K. & Coble, R. L., Solubilities of magnesia, titania, and magnesium titanate in aluminium oxide. *J Amer. Ceram. Soc.*, **51** (1968) 1–6.
5. Dorre, E. & Hubner, H., *Alumina: Processing, Properties, and Applications*. Springer-Verlag, 1984, p. 49.
6. Bagley, R. D., Cutler, I. B. & Johnson, D. L., Effect of TiO_2 on initial sintering of Al_2O_3. *J. Amer. Ceram. Soc.*, **53** (1970) 136–41.
7. Gitzen, W. H., *Alumina as a Ceramic Material*. The American Ceramic Society, OH, 1970, pp. 131–4.
8. Rabe, T., Nobst, P. & Moser, B., Phasenbestand und Sinterverhalten von Mn–Ti-dotierter Al_2O_3-Keramik in Abhängigkeit von der Sinteratmosphare. *Silikattechnik*, **34** (1983) 49–52.
9. Cahoon, H. P. & Christensen, C. J., Sintering and grain growth of alpha-alumina. *J. Amer. Ceram. Soc.*, **39** (1956) 337–44.
10. Cutler, I. B., Nucleation and nuclei growth in sintered alumina. In *Kinetics of High Temperature Processes.*, ed. W. D. Kingery. MIT Press, Cambridge, MA, 1959, pp. 120–7.
11. Keski, J. R. & Cutler, I. B., Effect of manganese oxide on sintering of alumina. *J. Amer. Ceram. Soc.*, **37** (1954) 653–4.
12. Keski, J. R. & Cutler, I. B., Initial sintering of Mn_xO–Al_2O_3. *J. Amer. Ceram. Soc.*, **51** (1968) 440–4.
13. Kostic, E., Kiss, S. J. & Boskovic, S., Sintering and microstructure development in the Al_2O_3—MnO—TiO_2 system. *Pow. Met. Int.*, **22** (1990) 29–30.
14. Leven, E. M., Robbins, C. R., McMurdie, H. F. & Reser, M. K., *Phase Diagrams for Ceramics* (ed.), 4th printing. The American Ceramic Society, 1979, p. 114.
15. Kingery, W. D., Bowen, H. K. & Uhlmann, D. R., *Introduction to Ceramics*. 2nd edn, John Wiley & Sons, 1976, p. 479.